Elucidating the Key Role of pH on Light-Driven Hydrogen Evolution by a Molecular Cobalt Catalyst

*Mirco Natali**

Department of Chemical and Pharmaceutical Sciences, University of Ferrara, Via Fossato di Mortara 17-19, 44121 Ferrara, Italy.

ABSTRACT

Photochemical hydrogen generation from aqueous solutions can be accomplished with a combination of at least three molecular components, namely a photosensitizer, a hydrogen evolving catalyst, and an electron donor. A parameter that plays a key role in the light-to-hydrogen efficiency of such three-component systems is the solution pH. While this evidence has been usually observed in several works aiming at identifying novel catalysts and optimizing their performances, detailed studies capable of shining light on this issue have been extremely rare. Hence the pH dependence of a reference three-component system based on $Ru(bpy)_3^{2+}$ (where bpy = 2,2'-bipyridine) as the sensitizer, a cobaloxime HEC, and ascorbic acid as the sacrificial donor has been studied with care by merging photocatalytic hydrogen evolution kinetic data and detailed time-resolved spectroscopy results. The photocatalytic activity shows a bell-shaped profile as a function of pH which peaks at around pH 5. While at acidic pH (pH < 5) the hydrogen evolving activity is limited by the photogeneration of reduced sensitizer species, at neutral to basic pH (pH > 5) the production of hydrogen is hampered by the disfavored protonation of the reduced Co(I) species. In this latter instance, however, hydrogen evolution is mainly slowed down rather than inhibited, as it is instead in the former case. This evidence has profound impact on the time scale of the photocatalysis and gives the opportunity to rationalize and correlate different results obtained with the same cobaloxime catalyst but under rather diverse experimental conditions.

KEYWORDS.

Hydrogen, water splitting, photocatalysis, cobaloxime, time-resolved spectroscopy.

INTRODUCTION

Production of hydrogen via proton reduction by photochemical means is by far recognized as a fundamental reaction which may provide, once coupled with water oxidation, a possible way for the generation of a clean fuel for a sustainable development.[1,2,3,4,5,6] Molecular systems can in principle accomplish this task providing also a large degree of tunability toward the optimization of this reductive half-reaction. Importantly, in the presence of a suitable proton source a combination of at least three basic components is required (Scheme 1), namely a hydrogen evolving catalyst (HEC), a photosensitizer (P), and an electron donor (D).[7,8,9,10,11]

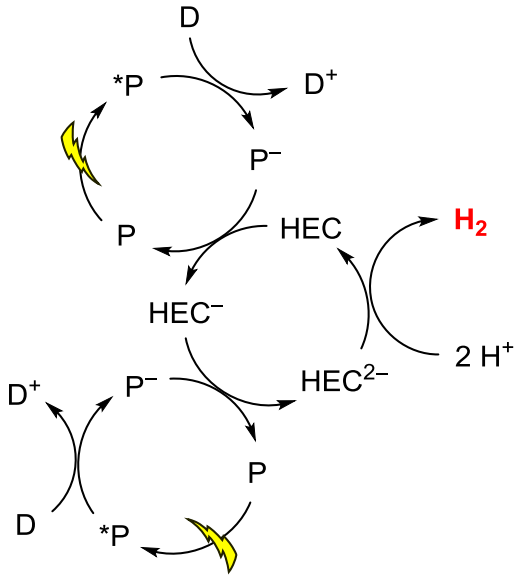

Scheme 1. Minimum set of components and reaction scheme of a photocatalytic hydrogen evolution system. Abbreviations: HEC = hydrogen evolving catalyst, P = photosensitizer, D = electron donor.

Among the HECs molecular species based on Earth-abundant metal centers have received considerable attention such as (i) cobalt complexes based on macrocyclic ligands,[12,13,14,15] including cobaloximes[16,17,18,19,20,21,22,23] and cobalt diimine-dioximes,[24,25] and polypyridine

ones,[26,27,28,29,30,31,32,33,34,35,36,37] (ii) iron polypyridine complexes[38,39] and molecular models of the natural [Fe,Fe]-hydrogenase,[40,41] and (iii) nickel complexes based on phosphine ligands (usually known as 'DuBois' catalysts).[42,43,44,45] Most of these catalysts have been studied in combination with different photosensitizers such as metal complexes,[16,17,20,26-36] porphyrins,[11,21-23] and more generally organic triplet sensitizers,[18,38,39] and sacrificial electron donors like aliphatic amines (TEA or TEOA)[16-18,20,23,33,38,39] and ascorbic acid.[13,15,21,26-32,34-36,43-45] Interestingly, in spite of the different experimental conditions usually employed for the characterization of such three-component systems the photochemical hydrogen evolution performances, both on a TON and TOF basis, were always found to be strongly pH dependent, typically featuring a pH optimum. While this behavior was usually rationalized considering a combination of different factors playing concomitantly and affecting the processes involved within the photoreaction mechanism (Scheme 1), no detailed studies were actually performed in order to deeply explain the dependence of photocatalytic hydrogen evolution on pH. Only recently, Reisner, Durrant, and coworkers reported[46] on the correlation between the hydrogen evolving activity and spectroscopic results unraveling the pH dependence of a three-component system based on a ruthenium sensitizer, ascorbic acid as the sacrificial donor, and a nickel 'DuBois' catalyst. The conclusions arising from this work, however, are mainly limited to the nickel-based system and no general extension to other photochemical systems can be thus done. Hence, in an attempt to shine more light onto the pH dependence of the HER within photocatalytic systems and to attain a more general picture potentially applicable to different catalysts, a reference three-component system[47] was chosen based on a ruthenium tris(bipyridine) complex as the light-harvesting sensitizer (**Ru**), a cobaloxime complex (**Co**) as the HEC, and ascorbic acid (**H_2A**) as the sacrificial electron donor (Chart 1) and analyzed it in detail. A convergent approach was adopted,

based on the systematic evaluation of the kinetics of the proton-coupled electron transfer (PCET) processes involved and the hydrogen evolution performances as a function of the pH. The results obtained allow for a better understanding of the effect of pH on photochemical hydrogen evolution by cobalt complexes and more generally molecular catalysts thus highlighting the importance of monitoring such a reaction parameter in order to improve the HER performances. Finally, these data give also a tool to rationalize some different behaviors observed in the literature concerning similar three-component systems devoted to light-driven hydrogen production.

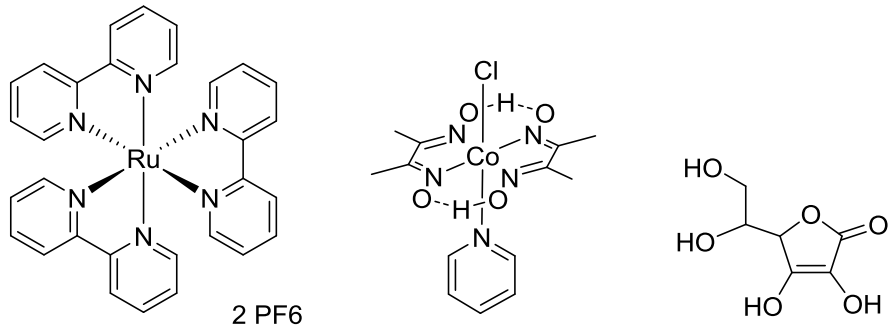

Ru **Co** **H_2A**

Chart 1. Molecular structure of the compounds used in this work.

EXPERIMENTAL SECTION

Materials. Spectroscopic grade acetonitrile was used for the spectroscopic and photolysis experiments and purchased from Sigma-Aldrich. Milli-Q Ultrapure water was used. Ascorbic acid and all other reagents were purchased from Sigma-Aldrich and used as received. The tris(2,2'-bipyridine)ruthenium(II) dihexafluorophosphate (**Ru**) and the cobaloxime (**Co**) complexes were available from previous studies.[47]

Apparatus and procedures. UV-Vis absorption spectra were recorded on a Jasco V-570 UV/Vis/NIR spectrophotometer. Emission spectra were taken on an Edinburgh Instrument

spectrofluorimeter equipped with a 900 W Xe arc lamp as excitation source, a photomultiplier tube, and an InGaAs detector for the visible and the NIR detection, respectively. Nanosecond transient absorption and time-resolved emission measurements were performed with a custom laser spectrometer comprised of a Continuum Surelite II Nd:YAG laser (FWHM = 8 ns) with frequency doubled, (532 nm, 330 mJ) or tripled (355 nm, 160 mJ) option, an Applied Photophysics Xe light source including a mod. 720 150 W lamp housing, a mod. 620 power controlled lamp supply and a mod. 03 - 102 arc lamp pulser. Laser excitation was provided at 90° with respect to the white light probe beam. Light transmitted by the sample was focused onto the entrance slit of a 300 mm focal length Acton SpectraPro 2300i triple grating, flat field, double exit monochromator equipped with a photomultiplier detector (Hamamatsu R3896). Signals from the photomultiplier (kinetic traces) were processed by means of a TeledyneLeCroy 604Zi (400 MHz, 20 GS/s) digital oscilloscope. Before all the spectroscopic measurements the solutions were purged with nitrogen for 10 minutes.

The hydrogen evolution experiments were carried out upon continuous visible light irradiation with a 175 W Xe arc-lamp (CERMAX PE175BFA) of a reactor containing the solution (a 10 mm pathlength pyrex glass cuvette with head space obtained from a round-bottom flask). A cut-off filter at $\lambda < 400$ nm and a hot mirror (IR filtering) have been used to provide the useful wavelength range (400-800 nm). The gas phase of the reaction vessel was analyzed on an Agilent Technologies 490 microGC equipped with a 5 Å molecular sieve column (10 m), a thermal conductivity detector, and using Ar as carrier gas. Additional details of the setup used for the photochemical hydrogen evolution experiments can be found in previous reports.[36,47] In a typical photocatalytic experiment, samples of 5 mL were prepared in 20 mL scintillation vials starting from **Ru** (0.25 mL from a 0.01 M mother solution in acetonitrile), and further adding **Co**

(small aliquots, typically between 0.1-0.2 mL, from a concentrated mother solution in acetonitrile), acetonitrile (depending on the amount of **Co** solution employed), water (2.5 mL), and finally **H_2A** and $NaH_2PO_4 \cdot H_2O$ (both as solid) to provide concentrations of 0.1 M and 0.01 M, respectively. The pH was adjusted to the required value upon addition of NaOH from a 5 M stock solution (changes in volume and concentration can be considered negligible, ≤ 2% dilution as estimated by absorption spectroscopy). The solution was then put in the reactor, degassed by bubbling Ar for 20 min, and thermostated at 18°C. The cell was then irradiated and the solution continually stirred during the photolysis. The gas phase of the reaction was analyzed through GC and the amount of hydrogen quantified.

RESULTS AND DISCUSSION

In order to study the effect of the pH on the hydrogen evolving ability of the three-component system herein considered the same experimental conditions as previously reported[47] were adopted, namely 0.5 mM **Ru**, 0.1 mM **Co**, 0.1 M **H_2A**, 50/50 acetonitrile/water. Only a small amount of $NaH_2PO_4 \cdot H_2O$ (0.01 M) was added in order to provide sufficient buffering capacity to the three-component mixture in 50/50 acetonitrile/water at neutral pH values without considerably altering the ionic strength of the solution (which is known to affect the bimolecular electron transfer kinetics).[48] Under these experimental conditions, the hydrogen evolution mechanism is expected to follow a reductive quenching pathway (Scheme 1) whereby, upon excitation, the **Ru** sensitizer undergoes reductive quenching by the **H_2A** with subsequent electron transfer from the photogenerated **Ru^-** species to the **Co** catalyst.[47]

Effect of pH on the reductive quenching.

The oxidation of ascorbic acid in aqueous solutions has been a subject of extensive research in the past[49,50,51,52,53,54,55] and it has been shown to be extremely pH dependent. Ascorbic acid is indeed a diprotic acid with two dissociation equilibria (eq 1,2) featuring pK_a of 4.1 and 11.8, respectively.[56]

$$\mathbf{H_2A} + H_2O \leftrightarrow \mathbf{HA^-} + H_3O^+ \qquad pK_a = 4.1 \qquad (1)$$

$$\mathbf{HA^-} + H_2O \leftrightarrow \mathbf{A^{2-}} + H_3O^+ \qquad pK_a = 11.8 \qquad (2)$$

Thus, depending on the pH ascorbic acid may be present as $\mathbf{H_2A}$, $\mathbf{HA^-}$, and $\mathbf{A^{2-}}$ and oxidation then occurs according to eq 3-5. The redox potentials for these one-electron transfer processes have been estimated as E = +1.17 V, +0.71 V, and +0.01 V vs. NHE, respectively.[54,55,57]

$$\mathbf{H_2A^{\bullet +}} + e^- \leftrightarrow \mathbf{H_2A} \qquad E = +1.17 \text{ V vs. NHE} \qquad (3)$$

$$\mathbf{HA^\bullet} + e^- \leftrightarrow \mathbf{HA^-} \qquad E = +0.71 \text{ V vs. NHE} \qquad (4)$$

$$\mathbf{A^{\bullet -}} + e^- \leftrightarrow \mathbf{A^{2-}} \qquad E = +0.01 \text{ V vs. NHE} \qquad (5)$$

The radical species produced by the one-electron transfer process in eq 3,4 are strong acids with dissociation constant of ca −4 and −0.86, respectively (eq 6,7).[51,55,56]

$$\mathbf{H_2A^{\bullet +}} + H_2O \leftrightarrow \mathbf{HA^\bullet} + H_3O^+ \qquad pK_a \approx -4 \qquad (6)$$

$$\mathbf{HA^\bullet} + H_2O \leftrightarrow \mathbf{A^{\bullet -}} + H_3O^+ \qquad pK_a = -0.86 \qquad (7)$$

Accordingly, regardless of the speciation of the ascorbic acid the one-electron oxidation almost quantitatively brings to the formation of the ascorbate radical ($\mathbf{A^{\bullet -}}$). This free radical species is not stable in aqueous solution and undergoes disproportionation (eq 8) with a bimolecular rate constant of $k = \sim 8 \cdot 10^7$ $M^{-1}s^{-1}$ yielding ascorbate and dehydroascorbic acid,[51,52] with the former ready to enter a new oxidation process. This reaction does explain why oxidation of ascorbic acid is overall a two-electron process and is actually of fundamental importance in the exploitation of such a molecule as a sacrificial electron donor.

$$2\,\mathbf{A}^{\bullet -} + H^{+} \leftrightarrow \mathbf{HA}^{-} + \mathbf{A} \qquad (8)$$

But now let us concentrate on the first electron transfer process which is of particular relevance within the photoreaction mechanism (Scheme 1). The triplet excited state of the ruthenium sensitizer **Ru** (E = +1.08 V vs. NHE)[47,58] may indeed play the role of one-electron oxidant and thus promote the reactions in eq 3-5. As a matter of fact, an earlier work reported the feasibility of the bimolecular quenching of the triplet excited state of **Ru** by ascorbic acid in aqueous solution at pH 4 with a rate constant of $k = 2 \cdot 10^7$ $M^{-1}s^{-1}$.[59] More recently, Schmehl and coworkers revisited the bimolecular excited state quenching of **Ru** by ascorbic acid in aqueous solution at different pH showing a variation of only a factor of 2 in the rate constant over a pH range between 3 and 8. Consistently, the amount of photogenerated $\mathbf{Ru}^{-}$ species by reductive quenching turned out to be almost pH independent.[56] Contrasting findings were, on the other hand, cast by Reisner, Durrant, and coworkers in their recent report on the pH effect of photochemical hydrogen evolution by a nickel catalyst showing remarkable pH dependence of the yield of photogenerated $\mathbf{Ru}^{-}$.[46]

In an attempt to get a deeper insight into this issue and in order to check whether the change of solvent from purely aqueous solution to a 50/50 acetonitrile/water mixture could cause variation in the quenching efficiency, the reductive quenching of excited **Ru** by $\mathbf{H_2A}$ and its pH dependence was investigated in detail. The emission of **Ru** (50 μM) in nitrogen purged 50/50 acetonitrile/water is quenched in the presence of 0.1 M $\mathbf{H_2A}$ with a strong pH dependence (Figure S1a), the quenching is almost completely dynamic as detected from the time-resolved emission kinetics (Figure S1b) consistent with a fully bimolecular process. A closer inspection into the pH dependence of the reductive quenching of the triplet excited state of **Ru** by ascorbic acid shows that the electron transfer rate increases by more than one order of magnitude with

increasing pH from 2 up to ca 4.5 and then becomes almost pH independent (Figure 1a). Interestingly, the trend of the I_0/I or τ_0/τ ratios qualitatively parallels the speciation of the ascorbate anion **HA**$^-$ in aqueous solution (Figure 1b).[60,61] This is in agreement with the lower driving force for the one-electron oxidation of the ascorbic acid **H$_2$A** than for the oxidation of the ascorbate anion **HA**$^-$ (see redox potential above) and with the hypothesis that the kinetics of the reductive electron transfer quenching process is limited by the deprotonation of **H$_2$A** (eq 1).

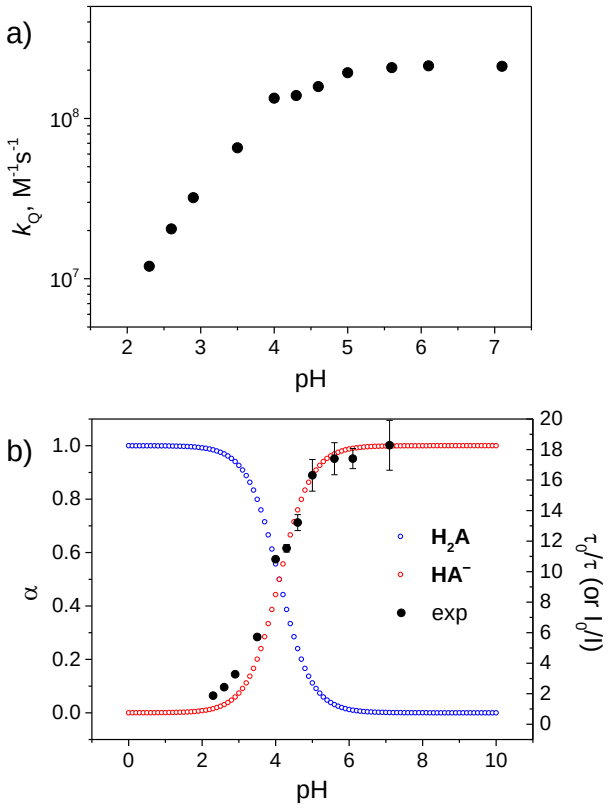

Figure 1. (a) Rate constant of the bimolecular reductive quenching of ascorbic acid as a function of pH; (b) trend of the τ_0/τ or I_0/I ratios with respect to the speciation of ascorbic acid (the second dissociation process has been herein neglected). Experimental conditions: 50 μM **Ru**, 0.1 M **H$_2$A**, 0.01 M $NaH_2PO_4 \cdot H_2O$, 50/50 acetonitrile/water, pH changed with NaOH.

Indeed, once the pH is sufficiently higher (above ca 4.5) than the first pK_a (eq 1), ascorbic acid almost exists as ascorbate anion only and its oxidation by the excited **Ru** sensitizer becomes easier from a thermodynamic viewpoint and thus faster (k = ~$2 \cdot 10^8$ $M^{-1}s^{-1}$). Interestingly, the observation that the reductive quenching rates at pH > 4.5 are practically independent of pH is consistent with the hypothesis that the proton-coupled oxidation of the ascorbate anion (eq 4,7) by ^{3}***Ru** occurs as a stepwise ET-PT (electron transfer - proton transfer) process wherein the electron transfer step (eq 4) is rate determining.

The reductive quenching of the **Ru** triplet excited manifold by ascorbic acid is followed by the generation of the reduced $\mathbf{Ru}^-$ species. Its formation and evolution in time can be detected by time-resolved absorption spectroscopy in the ns to μs time-scale since the $\mathbf{Ru}^-$ species displays a peculiar absorption at ca 510 nm.[27-36,46,47,56] Figure 2a display the kinetic traces at 510 nm obtained by laser flash photolysis on 50/50 acetonitrile/water mixtures at different pH containing 50 μM **Ru** and 0.1 M $\mathbf{H_2A}$. It is apparent that the amount of photogenerated $\mathbf{Ru}^-$ increases with increasing pH reaching a plateau at pH ≥ 4 with an overall yield (η_{Ru^-})[62,63,64,65] that directly parallels the trend observed in the quenching efficiency as a function of pH (Figure 2b and see Table S1 for the precise data). Interestingly, cage escape yields close to unity can be estimated at every pH examined (Table S1), consistent with the values observed in pure water,[56] a result that still confirms that the yield of photogenerated $\mathbf{Ru}^-$ species is directly dependent on the quenching efficiency and thus on the rate limiting deprotonation of $\mathbf{H_2A}$. It is worth noticing that, although the present investigation has been performed in a 50/50 acetonitrile/water mixture rather than in pure water, the data obtained seem more in agreement with the findings by Reisner, Durrant, and coworkers[46] than those by Schmehl and coworkers.[56] The reasons at the basis of these differences are presently unclear, although the use of additional concentrated

electrolytes in the latter case than in the former and the present cases (and the resulting ionic strength effect on the bimolecular ET processes)[48] could be a possible explanation.

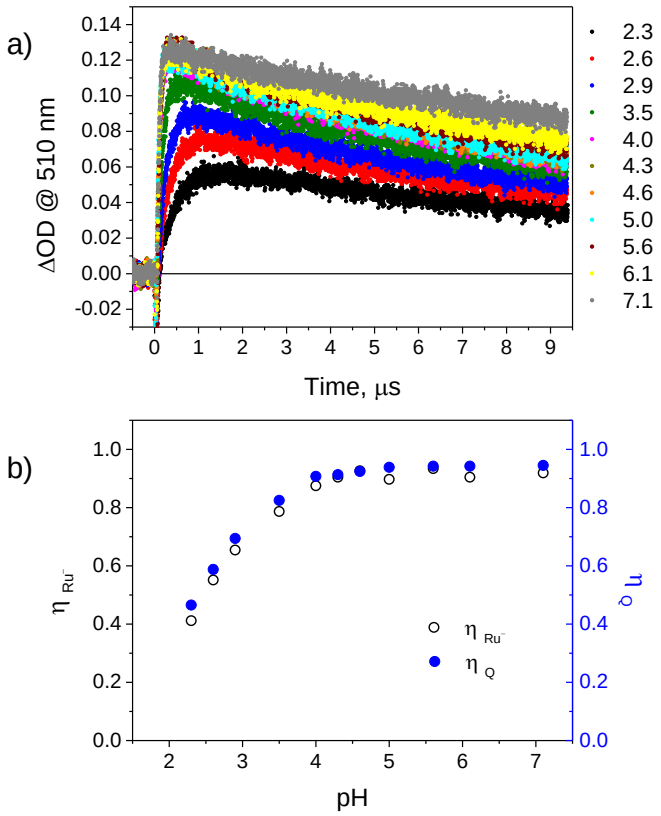

Figure 2. (a) Kinetic traces at 510 nm obtained by laser flash photolysis (excitation at 532 nm) of 50/50 acetonitrile/water solutions at different pH containing 50 μM **Ru**, 0.1 M **H_2A**, and 0.01 M $NaH_2PO_4 \cdot H_2O$; (b) trend of formation yield of **Ru^-** (η_{Ru^-}) and quenching yield (η_Q) as a function of pH.

In the absence of the **Co** catalyst the photogenerated **Ru^-** undergoes bimolecular charge recombination with the oxidized ascorbate radical.[47,56] This process can be monitored and time-resolved by following the kinetic traces at 510 nm on a longer time-scale and the rate constant of the bimolecular charge recombination step can be estimated according to a second-order kinetic treatment (Figure 3a). The kinetics are apparently pH dependent with rate constants which

decrease as the pH is increased over the investigated range (between 2 and 7, Figure 3b). The pH effect on charge recombination is, however, much weaker than for charge separation (a 4-fold larger slope is indeed obtained for charge separation than for charge recombination from the plot of the log *k* vs. pH). Since the reduction of the ascorbate radical $\mathbf{A}^{\bullet -}$ should involve both ET and PT processes to give $\mathbf{HA}^-$ or $\mathbf{H_2A}$, according to the redox and acid-base equilibria of ascorbic acid (see above), the weak pH dependence points towards the hypothesis that for charge recombination the PT events are most likely not the rate limiting steps.

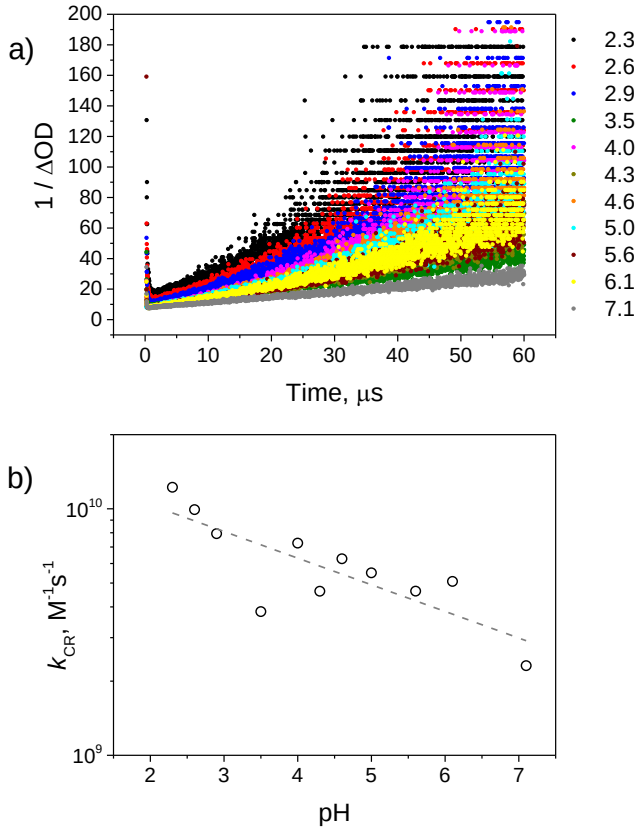

Figure 3. (a) Second-order kinetic treatment of the kinetic traces at 510 nm obtained by laser flash photolysis (excitation at 532 nm) of 50/50 acetonitrile/water solutions at different pH containing 50 μM **Ru**, 0.1 M $\mathbf{H_2A}$, and 0.01 M $NaH_2PO_4 \cdot H_2O$; (b) plot of the bimolecular rate constant for charge recombination vs. pH.

Effect of pH on the catalyst activation.

In the donor/sensitizer/catalyst three-component system, the reduced sensitizer **Ru**$^{-}$, once prepared via photoinduced reductive quenching by ascorbic acid, undergoes electron transfer to the cobalt catalyst in competition with charge recombination thus triggering the HER mechanism. As recently pointed out,[47] in the presence of excess ascorbic acid the cobaloxime catalyst (**Co**) is thermally reduced from a cobalt(III) species to a cobalt(II) one with concomitant loss of the axial chloride ligand, leaving a five-coordinated species with a free position potentially available for the coordination of the proton substrate.[66,67] Accordingly, the reduced photosensitizer should be actually responsible for the generation of a formal cobalt(I) species upon electron transfer (eq 9) which then can be protonated to yield the **Co**(III)-H intermediate required for the HER catalysis (eq 10).[68,69,70]

$$\mathbf{Ru}^{-} + \mathbf{Co}(\mathrm{II}) \rightarrow \mathbf{Ru} + \mathbf{Co}(\mathrm{I}) \qquad (9)$$

$$\mathbf{Co}(\mathrm{I}) + \mathrm{H}^{+} \leftrightarrow \mathbf{Co}(\mathrm{III})\text{-H} \qquad (10)$$

In order to follow the effect of pH on the catalyst activation step (eq 9,10) time-resolved absorption experiments were thus performed on 50/50 acetonitrile/water mixtures containing 50 μM **Ru**, 0.1 M $\mathbf{H_2A}$, 0.01 M $NaH_2PO_4 \cdot H_2O$. With the addition of small aliquots of concentrated NaOH the pH was changed over the range 2-9. In Figure 4 the spectral changes obtained by laser flash photolysis at three different pH values are reported. In all cases the first spectrum reported (0.5 μs time delay) is compatible with the reduced **Ru**$^{-}$ species, generated upon reductive quenching of excited **Ru** by ascorbic acid with the pH-dependent efficiencies reported above (Figure 2). The subsequent spectral evolution is, however, different. Qualitatively similar behavior is observed at pH 3.2 and 5.0 (Figure 4a,b, respectively), differing only in terms of

kinetics (see below), with the absorption band of the reduced **Ru**$^{-}$ species at ca 510 nm decaying monotonically towards the baseline without apparent formation of additional transient signals.

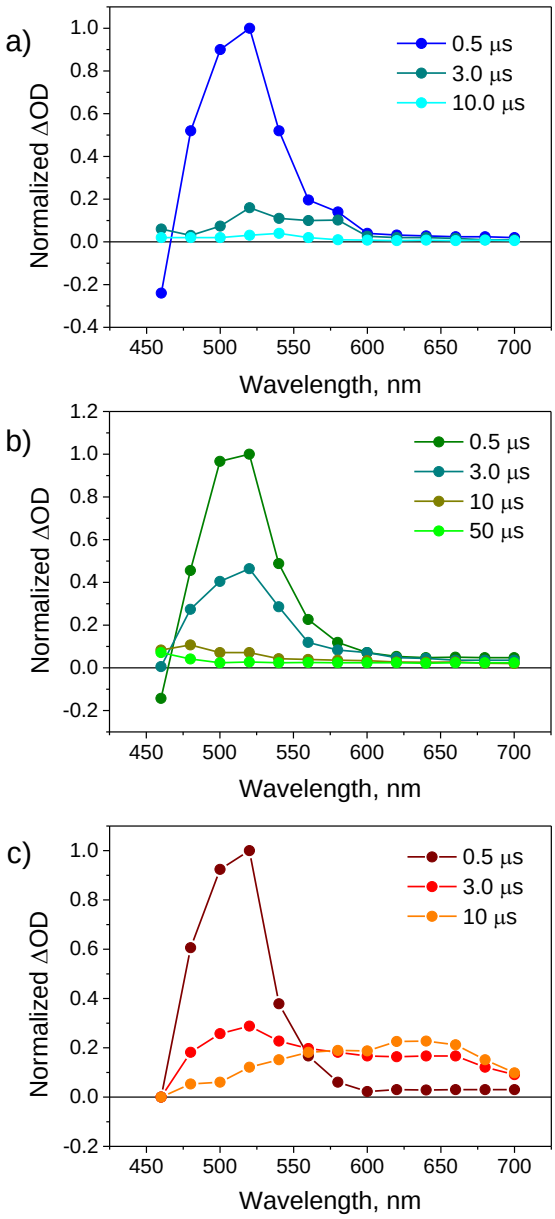

Figure 4. Transient spectra at different time-delays obtained by laser flash photolysis (excitation at 532 nm) of 50/50 acetonitrile/water solutions containing 50 µM **Ru**, 0.1 M **H_2A**, 0.01 M $NaH_2PO_4 \cdot H_2O$, and 0.1 mM **Co** (a) at pH 3.2, (b) at pH 5.0, and (c) at pH 9.2.

As previously inferred,[47] the observation that no additional transient signals, such as those typical of the **Co**(I) species,[16,71,72] develop following the decay of the reduced **Ru**$^-$ species speaks in favor of a PCET process with fast generation of the **Co**(III)-H intermediate, which is known to lack any appreciable absorption above 500 nm.[73,74] On the other hand, at pH 9.2 the transient spectrum of the reduced sensitizer starts decaying yet leaving a broad spectrum with maximum between 600-650 nm (isosbestic point at λ = 560 nm) which is fully compatible with the formation of a cobalt(I) species upon electron transfer from **Ru**$^-$ (eq 9).[16,71,72] This new spectrum then remains appreciably constant over a time window of 100 μs, suggesting that at this pH the protonation of **Co**(I) is not feasible.

In order to get a deeper understanding on the effect of pH on the mechanism of catalyst reduction the kinetic evolution of the transient spectra over the pH range 2-9 were followed at two different wavelengths, namely at 510 nm, to obtain information on the rate of the electron transfer from the **Ru**$^-$ species, and at 620 nm, to detect the amount of non-protonated **Co**(I) species formed.

In Figure 5 a plot is reported showing the pH dependence of both the observed decay rates (k_{obs}) of the photogenerated **Ru**$^-$ species, obtained by single-exponential fitting of the kinetic traces at 510 nm, and the related bimolecular rate constants (k_{ET}), obtained normalizing the observed rates by the **Co** concentration.[47] It should be pointed out that regardless of the pH all kinetics display a well-behaved first-order decaying profile (selected kinetic traces are shown in Figure S2) which is fully consistent with a single electron transfer event involving **Ru**$^-$ and **Co**(II) according to eq 9 (either followed or not by eq 10).[75] It is apparent that the ET rates are generally fast, close to the diffusion-controlled regime, and are appreciably pH dependent within the range 2-5 while becoming practically pH independent up to pH 9 (all the kinetic data are

reported in Table S2). A slight negative deviation is observed at highly acidic pH values, i.e., below pH 3, the reason is unknown but can be likely related to incomplete reduction of **Co**(III) to **Co**(II) by the ascorbic acid (increasing acidity is indeed expected to decrease its reduction ability, see above) or some decomposition of the cobaloxime moiety under those conditions.[76]

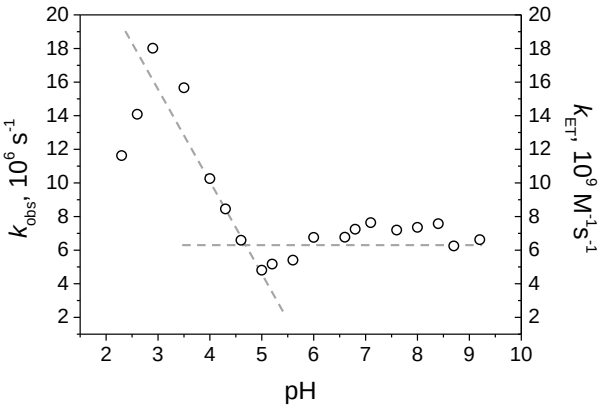

Figure 5. Plot of the observed rates (k_{obs}) and bimolecular rate constants (k_{ET}) for the decay of the **Ru**$^-$ vs. pH, calculated from the fitting of the kinetic traces at 510 nm obtained by laser flash photolysis experiment (excitation at 532 nm). Experimental conditions: 50 μM **Ru**, 0.1 M **H_2A**, 0.01 M $NaH_2PO_4 \cdot H_2O$, and 0.1 mM **Co**, 50/50 acetonitrile/water solutions, pH varied with NaOH.

In Figure 6a selected kinetic traces at 620 nm are reported while in Figure 6b the ΔOD at 620 nm sampled at 20 μs time-delay is plotted versus the solution pH. It can be noticed that the amount of detected **Co**(I) species is almost negligible at acidic pH, while it starts growing up from around pH 7 and practically plateaus at pH ≥ 9.

A thorough comparison between the results reported in Figure 5 and Figure 6b gives the opportunity to attain some detailed information as far as the catalyst activation step is concerned. At pH < 5 the absence of spectral signatures at 620 nm (see also the spectral variations in Figure

4a,b) is consistent with the fast generation of the **Co**(III)-H intermediate upon electron transfer from **Ru**$^{-}$ and protonation (eq 9,10). These observations, supported by the apparent pH dependence of the decaying rate of the **Ru**$^{-}$ spectral signature at 510 nm (Figure 5), strongly points towards a CPET (concerted proton-electron transfer) mechanism at the basis of the formation of the **Co**(III)-H species.[77] On the other hand, at pH > 5 the almost pH independent electron transfer rates (Figure 5) can be explained considering a change in the PCET mechanism from CPET to a step-wise ET-PT with a rate-determining ET process (eq 9).

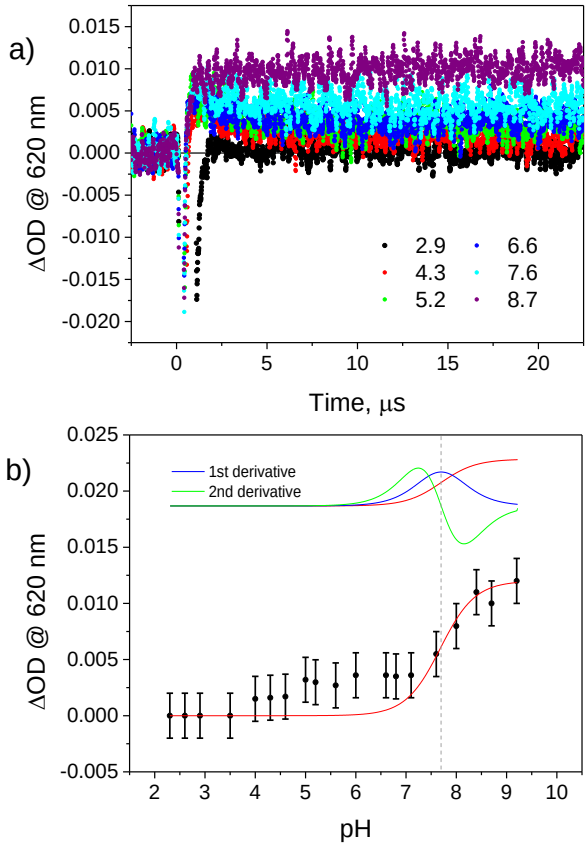

Figure 6. (a) Selected kinetic traces at 620 nm obtained by laser flash photolysis experiments (excitation at 532 nm) and (b) plot of the ΔOD at 620 nm vs. pH (1st and 2nd derivative of the sigmoidal fitting are reported in the inset). Experimental conditions: 50 μM **Ru**, 0.1 M **H_2A**, 0.01 M $NaH_2PO_4 \cdot H_2O$, and 0.1 mM **Co**, 50/50 acetonitrile/water solutions, pH varied with NaOH.

However, while in the pH range 5-7 the protonation step (eq 10) is almost quantitative, supporting the lack of appreciable transient signals at 620 nm (Figure 6), at pH > 7 the protonation equilibrium in eq 10 shifts progressively towards the non-protonated form, leaving substantial quantity of **Co**(I) species. Finally, at pH ≥ 9 the amount of **Co**(I) formed reaches a plateau suggesting that under these conditions the decay of the photogenerated $\mathbf{Ru}^{-}$ species is practically attributable to a simple ET process. Importantly, these results, not only allow for the identification of different PCET mechanisms, but in particular they give direct access to the acid-base equilibrium of the putative **Co**(III)-H intermediate (eq 10) relevant to the HER catalysis allowing for the determination of a $pK_a = 7.7$ under the experimental conditions used herein (see inset in Figure 6b). This is the first report where a pK_a of a Co(III)-hydride species has been determined by time-resolved spectroscopy. Interestingly, in spite of the different environment considered and techniques used, the estimated value falls in between the pK_a values determined theoretically by Muckerman and Fujita (4.17)[78] and by simulation of electrochemical data by Baffert, *et al*. (13.3).[79]

Effect of pH on photocatalytic hydrogen evolution.

Light-driven hydrogen evolution experiments were thus undertaken upon continuous visible irradiation of 50/50 acetonitrile/water solutions containing 0.5 mM **Ru**, 0.1 M $\mathbf{H_2A}$, 0.01 M $NaH_2PO_4 \cdot H_2O$, and 0.1 mM **Co** at different pH values over the range 3-8. The gas phase of the reaction was checked by gas chromatography (see Experimental Section). All the kinetic traces (average of two different experiments) are reported in Figure 7a (separated kinetics are reported in Figure S3-S8), while the pH dependence of both initial rate and maximum turnover frequency (TOF) is depicted in Figure 7b (relevant photolysis data are gathered in Table S3).[80] As it can be

observed from these data, the hydrogen evolving efficiencies show a bell-shaped profile, as typically observed in other three-component photochemical systems for hydrogen evolution,[16,21,28,34,44,46,81,82,83] which in this case displays a maximum at pH 5.

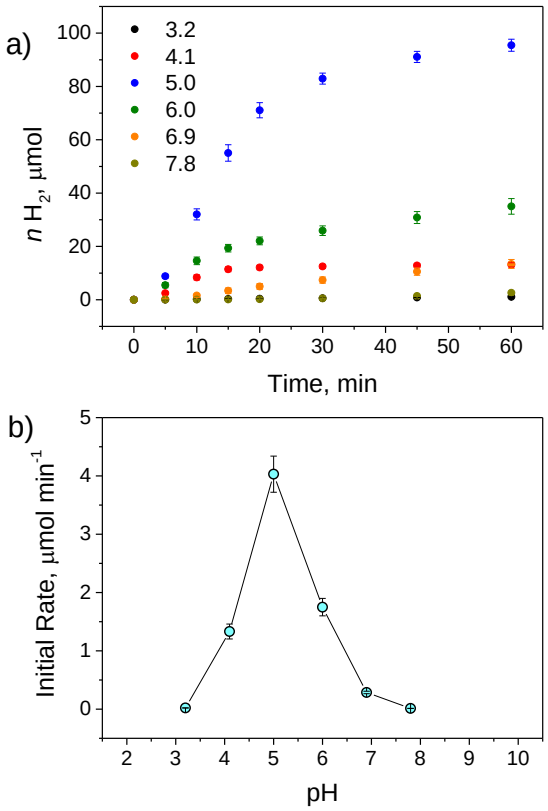

Figure 7. (a) Photocatalytic hydrogen evolution experiments and (b) pH dependence of the initial rate (estimated from a linear fit between 5-20 min). Experimental conditions: 0.5 mM **Ru**, 0.1 M **H_2A**, 0.01 M $NaH_2PO_4 \cdot H_2O$, and 0.1 mM **Co**, 50/50 acetonitrile/water solutions (5 mL), pH varied with NaOH.

Correlation between photolysis and spectroscopic data

The peak profile of the initial rate vs. pH as experimentally determined (Figure 7) can be rationalized considering the efficiencies of the PCET processes involved in the photoreaction mechanism and their pH dependence, as determined by transient absorption spectroscopy. The

decrease in the hydrogen evolving activity on going towards more acidic pH (pH < 5) can be attributed to the progressive decrease in the efficiency of the primary photochemical reaction, namely the photogeneration of reduced $\mathbf{Ru}^{-}$ sensitizer via reductive quenching by ascorbic acid (Figure 1).[46] As described above, the presence of an acid-base equilibrium for ascorbic acid with a pK_a = 4.1 (eq 1) and the slower reactivity of the associated $\mathbf{H_2A}$ than the dissociated $\mathbf{HA}^{-}$ species determines the decrease in the ^{3}***Ru** quenching yield and subsequent HER performance as long as the pH is lowered. On the other hand, the decrease in the hydrogen evolving efficiency with increasing pH (pH > 5) cannot be attributed to the photochemical reaction, which has comparable yields at pH values far beyond the first pK_a. The main issues are herein connected to the **Co** catalyst and its protonation ability. As a matter of fact, at more basic pH values the protonation of the **Co**(I) species, obtained by electron transfer from $\mathbf{Ru}^{-}$, becomes strongly disfavored. An estimated pK_a = 7.7 for the Co(I)/Co(III)-hydride equilibrium, as disclosed by time-resolved absorption measurements, can actually explain this situation.[84]

Interestingly, the optimum pH value for photoinduced hydrogen evolution obtained herein is comparable with the values recorded for other photocatalytic systems involving ruthenium tris(bipyridine) as the photosensitizer and ascorbic acid as the sacrificial donor, featuring values in the range 4-6 depending on the catalyst used.[28,34,46,56,82,83] While the decrease in photocatalytic activity below the optimum pH can be certainly related to the efficiency of the photochemical reaction involving the same sensitizer/donor couple (see above), the loss of performance above the optimum has to be connected with the type of catalyst used. In particular, in the case of cobalt HECs, the slight differences observed (pH optimum at 4 [ref 56,82], 4.5 [ref 83], between 5 and 6 [ref 28], or 5 [ref 34]) can be possibly attributed to the different electronic properties of the putative cobalt(I) catalytic intermediate and its proton affinity, while in the case of the water-

soluble nickel 'DuBois' catalyst (pH optimum at 4.5)[46] the reason for loss of hydrogen evolution activity above pH 4.5 has been mainly ascribed to the poor protonation of the pendant amine relays rather than the reduced metal center.

An interesting point also emerges once the hydrogen evolution kinetics at the most acidic pH (3.2) and at the most basic pH (7.8) tested are examined on a longer time scale (Figure S9). Both kinetics show similar, slow hydrogen evolution rates (0.021 and 0.013 μmol min^{-1} at pH 3.2 and 7.8, respectively), as estimated between 5-20 minutes after irradiation has started. However, while the hydrogen evolution at pH 3.2 almost levels off after 1 hour irradiation, the kinetics at pH 7.8 shows an induction period of about half an hour after that hydrogen production takes off with a larger rate (0.07 μmol min^{-1}, corresponding to a maximum TOF of 0.14 min^{-1}) and lasts longer, up to 4 hours irradiation. Not only, comparison of the absorption spectra before/after photolysis at the two different pH values (Figure S10 and S11) shows that at acidic pH hydrogen evolution is much more limited by sensitizer degradation than at basic pH. This may suggest that, the suppression of the primary photochemical process, namely reductive quenching of **Ru** by ascorbic acid, as it occurs at acidic pH (3.2) has negative effect on the sensitizer stability, with the chromophore likely undergoing photosubstitution reaction from thermally populated ^{3}MC *d-d* states in the presence of a large amount of ascorbic acid,[28] and therefore on the whole photochemical system. On the other hand, the disfavored protonation of **Co**(I) occurring at more basic pH (7.8) seems to preferentially slow down the hydrogen evolution catalysis rather than prevent it. Indeed, the presence of a quite long induction phase under these conditions can be consistent with a longer time required for an appreciable fraction of **Co**(II)-H, obtained by reduction of **Co**(III)-H, to accumulate at steady-state before a subsequent protonation step brings about hydrogen elimination. Interestingly, these pieces of evidence seem to support the different

behavior observed in **Co**-based three-component system for hydrogen evolution reported in the literature working under basic conditions (typically when aliphatic amines, such as TEA or TEOA, are used as the sacrificial electron donors instead of ascorbic acid).[16,85,86,87] Indeed, in such experiments the hydrogen evolution kinetics typically last longer, about 10-20 hours, yet being slower, with TOFs in the "h^{-1}" regime, with respect to those experiments performed under acidic conditions lasting usually few hours but showing TOFs in the "min^{-1}" regime.[21,47] Neglecting particular kinetic effects related to the sacrificial donor used (e.g., different reductive quenching rates, potential involvement of an oxidative quenching pathway, etc.), it can be argued that the change in the protonation equilibrium of the **Co**(I) species on passing from pH 4-6 (for experiments employing ascorbic acid as the sacrificial donor)[21,47] to pH 7-10 (for experiments using TEOA or TEA as the sacrificial donor)[16,85,86] may have a strong impact on the required time to accumulate substantial amount of **Co**(II)-H species by reduction of **Co**(III)-H and then in the overall photocatalysis time-scale thus providing a reasonable explanation of the two encountered kinetic regimes.

CONCLUSIONS

The pH dependence of the hydrogen evolution performance of a three-component system based on a cobaloxime HEC (**Co**), a ruthenium tris(bipyridine) sensitizer (**Ru**), and ascorbic acid (**H_2A**) as the sacrificial electron donor has been evaluated and compared with spectroscopic results obtained by time-resolved techniques. It has been shown that the bell-shaped profile of the hydrogen evolution rate with respect to pH, peaking at pH 5, is the result arising from a balance between two factors. In particular, the hydrogen evolution performance decreases as the pH is changed towards more acidic values (pH < 5) because of the lowering of the quenching

yield to reduce the excited **Ru** by the sacrificial donor. This is attributed to the presence of the acid-base equilibrium between ascorbic acid (**H_2A**) and ascorbate (**HA^-**) with $pK_a = 4.1$ with the former featuring considerably slower reactivity than the latter. On the other hand, the decrease in the hydrogen evolution efficiency with increasing pH towards more alkaline values (pH > 5) is ascribable to the disfavored protonation of the reduced **Co**(I), obtained by one-electron reduction by the photogenerated **Ru^-** species, owing to the presence of an acid-base equilibrium between **Co**(III)-H and **Co**(I) with a $pK_a = 7.7$. Interestingly, while the kinetic limiting factors at acidic pH are detrimental from a TON viewpoint, being responsible for sensitizer degradation, likely occurring by thermal population of the metal centered *d-d* states, the limiting factors at basic pH mainly slow down the hydrogen evolution photocatalysis. These observations may actually explain the remarkable differences observed in the time-scale of the photocatalytic experiments typically observed when photochemical systems employing ascorbic acid as the sacrificial donor are compared with those using aliphatic amines.

In conclusion, the understanding of the pH dependence of photocatalysis turns out to be a key point for the optimization of the hydrogen evolution performance. Although the operative pH range defined by this investigation is strictly related to the cobaloxime complex, the factors identified herein can be, on the other hand, potentially extended to all the class of molecular catalysts. It should be also pointed out that, while the pH effect related to the use of a certain sacrificial donor is of lesser importance in view of the utilization of sensitizer/catalyst couples in regenerative dye-sensitized photoelectrochemical cells (DS-PECs), the knowledge of the acid-base equilibrium of the metal-hydride catalytic intermediate appears to be of fundamental importance in order to drive the reductive half-reaction at a faster rate. Accordingly, larger

efforts towards this aim should be highly desirable and time-resolved spectroscopy techniques can thus be extremely helpful to solve such an important issue.

AUTHOR INFORMATION

Corresponding Author

* E-mail: mirco.natali@unife.it

Notes

The author declares no competing financial interests.

ASSOCIATED CONTENT

Supporting Information. Tables gathering both kinetic data of electron transfer processes and photolysis data, steady-state and time-resolved emission spectra of **Ru** in the presence of **H_2A** at different pH, selected kinetic traces at 510 nm on the three-component system, hydrogen evolution kinetics, comparison of absorption spectra before/after photolysis at pH 3.2 and 7.8. The following files are available free of charge.

ACKNOWLEDGMENT

Prof. Franco Scandola is gratefully acknowledged for helpful discussions and the critical reading of the manuscript. Financial support from the Italian MIUR (FIRB RBAP11C58Y ‘‘NanoSolar’’) is acknowledged.

REFERENCES

(1) Lewis, N. S.; Nocera, D. G. *Proc. Natl. Acad. Sci. U.S.A.* **2006**, *103*, 15729-15735.

(2) Gray, H. B. *Nat. Chem.* **2009**, *1*, 7.

(3) Armaroli, N.; Balzani, V.; Serpone, N. In *Powering Planet Earth: Energy Solutions for the Future*, Wiley, New York, 2012.

(4) Tachibana, Y.; Vayssieres, L.; Durrant, J. R. *Nat. Photon.* **2012**, *6*, 511-518.

(5) McKone, J. R.; Lewis, N. S.; Gray, H. B. *Chem. Mater.* **2014**, *26*, 407-414.

(6) Su, J.; Vayssieres, L. *ACS Energy Lett.* **2016**, *1*, 121-135.

(7) Andreiadis, E. S.; Chavarot-Kerlidou, M.; Fontecave, M.; Artero, V. *Photochem. Photobio.* **2011**, *87*, 946-964.

(8) Artero, V.; Chavarot-Kerlidou, M.; Fontecave, M. *Angew. Chem., Int. Ed.* **2011**, *50*, 7238-7266.

(9) Eckenhoff, W. T.; Eisenberg, R. *Dalton Trans.* **2012**, *41*, 13004-13021.

(10) Eckenhoff, W. T.; McNamara, W. R.; Du, P.; Eisenberg, R. *Biochim. Biophys. Acta* **2013**, *1827*, 958-973.

(11) Ladomenou, K.; Natali, M.; Iengo, E.; Charalampidis, G.; Scandola, F.; Coutsolelos, A. G. *Coord. Chem. Rev.* **2015**, *304-305*, 38-54.

(12) McCrory, C. C. L.; Uyeda, C.; Peters, J. C. *J. Am. Chem. Soc.* **2012**, *134*, 3164-3170.

(13) Varma, S.; Castillo, C. E.; Stoll, T.; Fortage, J.; Blackman, A. G.; Molton, F.; Deronzier, A.; Collomb, M.-N. *Phys. Chem. Chem. Phys.* **2013**, *15*, 17544-17552.

(14) Gimbert-Suriñach, C.; Albero, J.; Stoll, T.; Fortage, J.; Collomb, M.-N.; Deronzier, A.; Palomares, E.; Llobet, A. *J. Am. Chem. Soc.* **2014**, *136*, 7655-7661.

(15) Moonshiram, D.; Gimbert-Suriñach, C.; Guda, A.; Picon, A.; Lehmann, C. S.; Zhang, X.; Doumi, G.; March, A. M.; Benet-Buchholz, J.; Soldatov, A.; Llobet, A.; Southworth, S. H. *J. Am. Chem. Soc.* **2016**, *138*, 10586-10596.

(16) Du, P.; Knowles, K.; Eisenberg, R. *J. Am. Chem. Soc.* **2008**, *130*, 12576-12577.

(17) Fihri, A.; Artero, V.; Razavet, M.; Baffert, C.; Leibl, W.; Fontecave, M. *Angew. Chem., Int. Ed.* **2008**, *47*, 564-567.

(18) McCormick, T. M.; Calitree, B. D.; Orchard, A.; Kraut, N. D.; Bright, F. V.; Detty, M. R.; Eisenberg, R. *J. Am. Chem. Soc.* **2010**, *132*, 15480-15483.

(19) Dempsey, J. L.; Winkler, J. R.; Gray, H. B. *J. Am. Chem. Soc.* **2010**, *132*, 1060-1065.

(20) Lakadamyali, F.; Reynal, A.; Kato, M.; Durrant, J. R.; Reisner, E. *Chem. Eur. J.* **2012**, *18*, 15464-15476.

(21) Natali, M.; Argazzi, R.; Chiorboli, C.; Iengo, E.; Scandola, F. *Chem. Eur. J.* **2013**, *19*, 9261-9271.

(22) Natali, M.; Orlandi, M.; Chiorboli, C.; Iengo, E.; Bertolasi, V.; Scandola, F. *Photochem. Photobio. Sci.* **2013**, *12*, 1749-1753.

(23) Peuntinger, K.; Lazarides, T.; Dafnomili, D.; Charalambidis, G.; Landrou, G.; Kahnt, A.; Sabatini, R. P.; McCamant, D. W.; Gryko, D. T.; Coutsolelos, A. G.; Guldi, D. M. *J. Phys. Chem. C* **2013**, *117*, 1647-1655.

(24) Kaeffer, N.; Chavarot-Kerlidou, M.; Artero, V. *Acc. Chem. Res.* **2015**, *48*, 1286-1295.

(25) Willkomm, J.; Muresan, N.; Reisner, E. *Chem. Sci.* **2015**, *6*, 2727-2736.

(26) Sun, Y.; Sun, J.; Long, J. R.; Yang, P.; Chang, C. J. *Chem. Sci.* **2013**, *4*, 118-124.

(27) Nippe, M.; Khnayzer, R. S.; Panetier, J. A.; Zee, D. Z.; Olaiya, B. S.; Head-Gordon, M.; Chang, C. J.; Castellano, F. N.; Long, J. R. *Chem. Sci.* **2013**, *4*, 3934-3945.

(28) Khnayzer, R. S.; Thoi, V. A.; Nippe, M.; King, A. E.; Jurss, J. W.; El Roz, K. A.; Long, J. R.; Chang, C. J.; Castellano, F. N. *Energy Environ. Sci.* **2014**, *7*, 1477-1488.

(29) Bachmann, C.; Guttentag, M.; Spingler, B.; Alberto, R. *Inorg. Chem.* **2013**, *52*, 6055-6061.

(30) Singh, W. M.; Mirmohades, M.; Jane, R. T.; White, T. A.; Hammarström, L.; Thapper, A.; Lomoth, R.; Ott, S. *Chem. Commun.* **2013**, *49*, 8638-8640.

(31) Tong, L.; Zong, R.; Thummel, R. P. *J. Am. Chem. Soc.* **2014**, *136*, 4881-4884.

(32) Xie, J.; Zhou, Q.; Li, C.; Wang, W.; Hou, Y.; Zhang, B.; Wang, X. *Chem. Commun.* **2014**, *50*, 6520-6522.

(33) Leung, C.-F.; Ng, S.-M.; Ko, C.-C.; Man, W.-L.; Wu, J.; Chen, L.; Lau, T.-C. *Energy Environ. Sci.* **2012**, *5*, 7903-7907.

(34) Deponti, E.; Luisa, A.; Natali, M.; Iengo, E.; Scandola, F. *Dalton Trans.* **2014**, *43*, 16345-16353.

(35) Lo, W. K. C.; Castillo, C. E.; Gueret, R.; Fortage, J.; Rebarz, M.; Sliwa, M.; Thomas, F.; McAdam, C. J.; Jameson, G. B.; McMorran, D. A.; Crowley, J. D.; Collomb, M.-N.; Blackman, A. G. *Inorg. Chem.* **2016**, *55*, 4564-4581.

(36) Natali, M.; Badetti, E.; Deponti, E.; Gamberoni, M.; Scaramuzzo, F. A.; Sartorel, A.; Zonta, C. *Dalton Trans.* **2016**, *45*, 14764-14773.

(37) Queyriaux, N.; Jane, R. T.; Massin, J.; Artero, V.; Chavarot-Kerlidou, M. *Coord. Chem. Rev.* **2015**, *304-305*, 3-19.

(38) Cavell, A. C.; Hartley, C. L.; Liu, D.; Tribble, C. S.; McNamara, W. R. *Inorg. Chem.* **2015**, *54*, 3325-3330.

(39) Hartley, C. L.; DiRisio, R. J.; Screen, M. E.; Mayer, K. J., McNamara, W. R. *Inorg. Chem.* **2016**, *55*, 8865-8870.

(40) Tard, C.; Pickett, C. J. *Chem. Rev.* **2009**, *109*, 2245-2274.

(41) Lomoth, R.; Ott, S. *Dalton Trans.* **2009**, 9952-9959.

(42) Helm, M. L.; Stewart, M. P.; Bullock, R. M.; DuBois, M. R.; DuBois, D. L. *Science* **2011**, *333*, 863-866.

(43) McLaughlin, M. P.; McCormick, T. M.; Eisenberg, R.; Holland, P. L. *Chem. Commun.* **2011**, *47*, 7989-7991.

(44) Gross, M. A.; Reynal, A.; Durrant, J. R.; Reisner, E. *J. Am. Chem. Soc.* **2014**, *136*, 356-366.

(45) Weingarten, A. S.; Kazantsev, R. V.; Palmer, L. C.; McClendon, M.; Koltonow, A. R.; Samuel, A. P. S.; Kiebala, D. J.; Wasielewski, M. R.; Stupp, S. I. *Nat. Chem.* **2014**, *6*, 964-970.

(46) Reynal, A.; Pastor, E.; Gross, M.; Selim, S.; Reisner, E.; Durrant, J. R. *Chem. Sci.* **2015**, *6*, 4855-4859.

(47) Deponti. E.; Natali, M. *Dalton Trans.* **2016**, *45*, 9136-9147.

(48) Chiorboli, C.; Indelli, M. T.; Rampi Scandola, M. A.; Scandola, F. *J. Phys. Chem.* **1988**, *82*, 156-163.

(49) Pelizzetti, E.; Mentasti, E.; Pramauro, E. *Inorg. Chem.* **1976**, *15*, 2898-2900.

(50) Pelizzetti, E.; Mentasti, E.; Pramauro, E. *Inorg. Chem.* **1978**, *17*, 1181-1186.

(51) Bielski, B. H. J.; Comstock, D. A.; Bowen, R. A. *J. Am. Chem. Soc.* **1971**, *93*, 5624-5629.

(52) Bielski, B. H. J.; Allen, A. O.; Schwarz, H. A. *J. Am. Chem. Soc.* **1981**, *103*, 3516-3518.

(53) Cabelli, D. E.; Bielski, B. H. J. *J. Phys. Chem.* **1983**, *83*, 1809-1812.

(54) Creutz, C. *Inorg. Chem.* **1981**, *20*, 4449-4452.

(55) Macartney, D. H.; Sutin, N. *Inorg. Chem. Acta* **1983**, *74*, 221-228.

(56) Shan, B.; Baine, T.; Ma, X. A. N.; Zhao, X.; Schmehl, R. H. *Inorg. Chem.* **2013**, *52*, 4853-4859.

(57) It should be noticed that while the potential values of the oxidation of the ascorbate anion $\mathbf{HA^-}$ and dianion $\mathbf{A^{2-}}$ (eq 4,5) are consistent with experimental data,[51] the redox potential of the oxidation of ascorbic acid $\mathbf{H_2A}$ (eq 3) is the result of a theoretical calculation and should thus be taken with care.[52]

(58) Juris, A.; Balzani, V.; Barigelletti, F.; Campagna, S.; Belser, P.; Von Zelevsky, A. *Coord. Chem. Rev.* **1988**, *84*, 85-277.

(59) Creutz, C.; Sutin, N.; Brunschwig, B. *J. Am. Chem. Soc.* **1979**, *101*, 1298-1300.

(60) In the correlation between the quenching parameters and the speciation of ascorbic acid (Figure 1b) a pK_a = 4.1 has been assumed which is the value estimated in purely aqueous solution, although the present quenching measurements have been performed in a 50/50 acetonitrile/water mixture. No large variations between the actual pH and the measured one, however, should be expected in the presence of 50% acetonitrile in water[61] which makes the correlation reasonably acceptable.

(61) Gagliardi, L. G.; Castells, C. B.; Ràfols, C.; Rosés, M.; Bosch, E. *Anal. Chem.* **2007**, *79*, 3180-3187.

(62) Formation yield of the reduced $\mathbf{Ru^-}$ species have been calculated taking **Ru** as actinometer ($\Delta\varepsilon = -10{,}600\ M^{-1}cm^{-1}$ at λ = 450 nm and $\Phi_{isc} = 1$ for ^{3}*Ru),[63] then considering the

maximum ΔOD in the kinetic traces at different pH values (Figure 2a) and using a molar extinction coefficient of $\Delta\varepsilon = 9{,}000\ M^{-1}cm^{-1}$ at $\lambda = 510$ nm.[64,65]

(63) Creutz, C.; Chou, M.; Netzel, T. L.; Okumura, M.; Sutin, N. *J. Am. Chem. Soc.* **1980**, *102*, 1309-1319.

(64) Creutz, C.; Sutin, N. *J. Am. Chem. Soc.* **1976**, *98*, 6384-6385.

(65) Kelly, L. A.; Rodgers, M. A. J. *J. Phys. Chem.* **1994**, *98*, 6377-6385.

(66) Bhattacharjee, A.; Andreiadis, E. S.; Chavarot-Kerlidou, M.; Fontecave, M.; Field, M. J.; Artero, V. *Chem. Eur. J.* **2013**, *19*, 15166-15174.

(67) Solis, B. H.; Yu, Y.; Hammes-Schiffer, S. *Inorg. Chem.* **2013**, *52*, 6994-6999.

(68) Subsequent reduction and protonation of the **Co**(III)-H species are expected to promote hydrogen evolution, see, e.g., refs 69,70.

(69) Dempsey, J. L.; Brunschwig, B. S.; Winkler, J. R.; Gray, H. B. *Acc. Chem. Res.* **2009**, *42*, 1995-2004

(70) Rountree, E. S.; Martin, D. J.; McCarthy, B. D.; Dempsey, J. L. *ACS Catal.* **2016**, *6*, 3326-3335.

(71) Du, P.; Schneider, J.; Luo, G.; Brennessel, W. W.; Eisenberg, R. *Inorg. Chem.* **2009**, *48*, 4952-4962.

(72) Pantani, O.; Anxolabéhère-Mallart, E.; Aukauloo, A.; Millet, P. *Electrochem. Comm.* **2007**, *9*, 54-58.

(73) Creutz, C.; Schwarz, H. A.; Wishart, J. F.; Fujita, E.; Sutin, N. *J. Am. Chem. Soc.* **1991**, *113*, 3361-3371.

(74) Lewandowska-Andralojc, A.; Baine, T.; Zhao, X.; Muckerman, J. T.; Fujita, E.; Polyansky, D. E. *Inorg. Chem.* **2015**, *54*, 4310-4321.

(75) In fact, under the experimental conditions used the amount of **Co** catalyst (0.1 mM) far exceeds the quantity of photogenerated $\mathbf{Ru}^{-}$ species (≤ 10 μM). Accordingly, a pseudo-first order kinetic treatment is perfectly suitable for describing the observed first-order decaying kinetics.[56] This gives an electron transfer rate $r_{ET} = k_{ET}\,[\mathbf{Co}][\mathbf{Ru}^{-}] \approx k_{obs}\,[\mathbf{Ru}^{-}]$ with the observed rate $k_{obs} = k_{ET}\,[\mathbf{Co}]$ estimated from a single-exponential fitting from $\Delta OD(t) = \Delta OD(0)\exp(-k_{obs}\,t)$.

(76) Schrauzer, G. N. *Inorg. Synth.* **1968**, *11*, 61-70.

(77) An alternative, stepwise PT-ET mechanism can be clearly ruled out since it would require protonation of a Co(II) moiety which is extremely unlikely.

(78) Muckerman, J. T.; Fujita, E. *Chem. Commun.* **2011**, *47*, 12456-12458.

(79) Baffert, C.; Artero, V.; Fontecave, M. *Inorg. Chem.* **2007**, *46*, 1817-1824.

(80) It should be stressed that a straightforward correlation between the hydrogen evolving activity and the pH is meaningful only in terms of initial rate or maximum TOF, being directly related to the quantum yield of the photoreaction (which is based on the assumption that the kinetic of hydrogen evolution is appreciably dependent on the absorbed photons only), while other parameters, such as the turnover number (TON), are potentially affected by other external variables (rather than absorbed light only).

(81) Natali, M.; Luisa, A.; Iengo, E.; Scandola, F. *Chem. Commun.* **2014**, *50*, 1842-1844.

(82) McNamara, W. R.; Han, Z.; Alperin, P. J.; Brennessel, W. W.; Holland, P. L.; Eisenberg, R. *J. Am. Chem. Soc.* **2011**, *133*, 15368-15371.

(83) Tong, L.; Kopecky, A.; Zong, R.; Gagnon, K. J.; Ahlquist, M. S. G.; Thummel, R. P. *Inorg. Chem.* **2015**, *54*, 7873-7884.

(84) It should be mentioned that, as previously noticed, before hydrogen evolution takes place the following steps must occur: (i) reduction of **Co**(III)-H to **Co**(II)-H by photogenerated $\mathbf{Ru}^{-}$, (ii) protonation of **Co**(II)-H to a "formal" **Co**(II)-H_2 species, and (iii) hydrogen release. While process (iii) is thought to be pH independent,[70] the PCET reaction (processes (i) and (ii)) leading to the formation of the **Co**(II)-H_2 species may actually be affected by the pH. This reaction sequence is, however, difficult to characterize from an experimental point of view. This notwithstanding, it could be argued that, although the second protonation process (ii) is usually considered as the rate-limiting step of the HER catalysis under electrochemical conditions, under continuous photolysis the considerably small concentrations of both reducing agent[56] and **Co**(III)-H species are likely to make process (i) rate-determining. Within this hypothesis, the sequence of processes (i), (ii), and (iii) is thus expected to be overall weakly dependent on pH. The fact that the pH dependence of the photocatalysis at pH > 5 is substantially compatible with the pH dependence of the first PCET process (eq 9,10) seems to be consistent with this assumption.

(85) Lazarides, T.; McCormick, T. M.; Du, P.; Luo, G.; Lindley, B.; Eisenberg, R. *J. Am. Chem. Soc.* **2009**, *131*, 9192-9194.

(86) Lazarides, T.; Delor, M.; Sazanovich, I. V.; McCormick, T. M.; Georgakaki, I.; Charalambidis, G.; Weinstein, J. A.; Coutsolelos, A. G. *Chem. Commun.* **2014**, *50*, 521-523.

(87) Panagiotopoulos, A.; Ladomenou, K.; Sun, D.; Artero, V.; Coutsolelos, A. G. *Dalton Trans.* **2016**, *45*, 6732-6736.

SYNOPSIS.

The pH dependence of photochemical hydrogen evolution by a cobaloxime catalyst has been elucidated in detail by means of time-resolved spectroscopic techniques.